Segmental Dynamics in Bulk Poly(isobornyl methacrylate) and Its Random Copolymer with Poly(methyl methacrylate) near T_g

F. Alvarez and J. Colmenero*

Departamento de Física de Materiales, Universidad del País Vasco, 20080 San Sebastián, Spain

C. H. Wang and J. L. Xia

Department of Chemistry, University of Nebraska, Lincoln, Nebraska 68588-0304

G. Fytas

FORTH-IESL, P.O. Box 1527, Heraklion, Crete, Greece

Received December 20, 1994; Revised Manuscript Received June 22, 1995®

ABSTRACT: Relaxation processes of bulk poly(isobornyl methacrylate) (PIMA) and its 50% random copolymer with poly(methyl methacrylate) (PMMA) have been studied in the glass transition temperature region by means of photon correlation spectroscopy (PCS) and dielectric relaxation spectroscopy (DS). The experimental results were analyzed in a consistent way employing an inverse Laplace transform analysis of the time correlation function of density fluctuations and the dielectric relaxation spectroscopic data utilizing a recently developed algorithm. For bulk PIMA, the time correlation function clearly shows two distinct relaxation modes, whereas dielectric relaxation is dominated by the α-relaxation mode. The fast process detected in PCS is assigned to be the rotation arising from the rigid isobornyl group about the C–O bond. In the 50% random copolymer, DS displays a β-relaxation and a slower α-relaxation process, in agreement with the PCS results. Moreover, in PCS the time correlation function of density fluctuations shows strong evidence of a slow relaxation mode, which exhibits a narrow distribution of relaxation times. This mode is tentatively assigned to be arising probably from composition fluctuations in the copolymer. The molecular origin of these modes is discussed.

1. Introduction

Due to its optical transparency in the visible region and desirable mechanical properties, amorphous atactic poly(methyl methacrylate) (PMMA) is currently used for fiber-optics application. The glass transition temperature (T_g) of atactic PMMA is about 373 K. As a result, fiber-optics applications of PMMA are limited to about 353 K, above which PMMA fiber becomes soft and loses its mechanical integrity. However, by replacing the methyl group in the ester moiety with a bulky bicyclic isobornyl group, one obtains poly(isobornyl methacrylate) (PIMA), which may have a glass transition temperature as high as 423 K. The high T_g of PIMA is due in part to the difficulty of the isobornyl side group to undergo free rotation, thereby resulting in reduced chain flexibility.[1]

In addition to high T_g, PIMA is heat resistive and also exhibits superior optical transparency. However, our investigations of mechanical and optical properties of PIMA and poly(IMA–MMA) copolymers have shown that pure PIMA has a considerably smaller shear modulus and is more brittle than PMMA.[1] However, by blending or copolymerizing PIMA with PMMA, its mechanical property is considerably improved, yet without significantly affecting the optical property, due to the fact that the refractive indices of PIMA and PMMA are quite close. Consequently, the intensity loss due to light scattering for fibers made of a PIMA–PMMA blend or copolymer remains unchanged as compared to pure PMMA. The light scattering loss arising from composition inhomogeneity (or concentration fluctuations) is insignificant in the PIMA–PMMA blend and copolymer.

The dilute solution properties of PIMA were reported by Hadjichristidis et al.[2] using viscosimetry, size-exclusion chromatography (SEC), and static light scattering and recently using viscosimetry, SEC, and static and dynamic light scattering for high molecular weight ($>10^6$) PIMA in THF.[3] However, despite the potential application for fiber optics at higher temperature for IMA–MMA copolymers, there appears to be no report available in the scientific literature on the physical characterization of PIMA or IMA–MMA copolymer in the bulk state; preliminary results on PIMA were recently reported by the present authors.[4] To elucidate the type of motion involved in PIMA and IMA–MMA copolymer melts, we have carried out photon correlation spectroscopy (PCS) and dielectric spectroscopy (DS) studies of these samples. The primary (α) and secondary (β) relaxation processes arising from local segmental motions in bulk polymers can affect the density fluctuations and the dielectric susceptibility respectively probed by PCS and DS.

For bulk homopolymers, a consistent analysis of these observables led to the same relaxation function for the α-process.[5–7] For polymer blends and block copolymers, however, recent studies[8–10] have shown the presence of two α-relaxation processes even in the absence of thermodynamic interactions. Albeit the origin of this splitting is uncertain, it probably relates to the dynamic compatibility of the two components for local structural rearrangements involved in the glass dynamics, e.g., disparity in the cooperative lengths. The modification of the segmental dynamics in interacting polymer systems with different monomer structures is a new subject of current interest. For the present IMA–MMA system the dynamics of segmental motion of the main chain and the reorientation of the ester side group that bears the bulky isobornyl moiety in PIMA are found to

® Abstract published in *Advance ACS Abstracts*, August 15, 1995.

0024-9297/95/2228-6488$09.00/0

be sharply affected in the copolymer with 50 wt % PMMA. The result is compared with that obtained for bulk PMMA[11] previously published.

2. Experimental Section

Poly(isobornyl methacrylate) was prepared by a standard free-radical polymerization procedure. Pure MMA and IMA monomers were provided by Rohm & Haas Co. They were purified by vacuum distillation to remove inhibitor. Appropriate amounts of purified IMA and MMA were placed in a test tube, with 0.2 wt % of benzoyl peroxide initiator added to each tube. Test tubes containing monomers and initiator were flame-sealed and placed in an oven for controlled polymerization by a gradual temperature increase of 10 K every 24 h over a range extending from 313 to 433 K. Transparent rods free from the presence of monomer were obtained after 12 days of polymerization.

PCS measurements were performed with an argon ion laser (Spectra Physics 2020) operating at a wavelength of $\lambda = 488$ nm with a power of 150 mW. The incident and the scattered laser beam were both polarized perpendicular to the scattering plane, yielding the V_V component of the scattered intensity. The V_H component was found to be small; hence, the V_V component was practically associated with isotropic scattering. Intensity autocorrelation functions, $G(t)$, were measured in the time range of 10^{-6}–10^2 s, using an ALV-5000 correlator. The homodyne intensity correlation function $G(t)$ is related to the normalized density time correlation function $g(t)$ by

$$G(t) = A(1 + f|\alpha g(t)|^2) \quad (1)$$

where A is the baseline, f the instrumental factor (which was found to be 0.4 for the present system), and α the fraction of the total scattered intensity associated with the slow density fluctuations that lies inside the time window of the correlator.[12] The temperature range measured in this work was from 418 to 438 K for bulk PIMA and from 403 to 453 K for copolymer.

Measurements of dynamic susceptibility, $\epsilon^* = \epsilon' - i\epsilon''$, were carried out by means of an experimental setup which used a lock-in amplifier EG&G PAR 5208 equipped with an internal oscillator, allowing the dielectric response over the frequency range between 10 Hz and 100 kHz to be covered. The stray capacitance of the cell was reduced to 10^{-14} F. The sample was held between two condenser aluminum plates that were kept at a fixed distance. The capacitance of the sample cell was on the order of 10^{-11} F. A standard 10 pF air capacitor was used as a reference in order to minimize errors in dielectric loss measurements; the experimental limit for the loss factor value was about 10^{-4}. The measurements were performed by using frequency scans under an isothermal condition for the temperatures between 420 and 470 K for bulk PIMA and between 320 and 440 K for copolymer. The temperature dependence of the dielectric response at constant frequencies was measured from 460 K down to 100 K for the sample kept in a helium atmosphere. The glass transition temperatures T_g of the samples measured by differential scanning calorimetry with a constant heating rate of 10 K/min were 396 K for bulk PIMA and 380 K for the copolymer.

3. Data Analysis

The field autocorrelation function, $\alpha g(t)$, was obtained from the intensity autocorrelograms, $G(t)$, in accordance with eq 1. After removing the instrumental factor f, it was directly inserted in the CONTIN[13] program to obtain the distribution function of relaxation times $\varrho(\ln \tau)$ as follows:

$$\alpha g(t) = \int_{-\infty}^{\infty} \varrho(\ln \tau) \exp(-t/\tau)\, d \ln \tau \quad (2)$$

The same procedure was carried out using our modified version of CONTIN for the frequency domain to obtain $\varrho(\ln \tau)$ from the measured dielectric loss peak. This modified version uses an algorithm in the frequency domain. The basic idea lies on the ground that, if the dielectric relaxation function in the time domain can be expressed as a continuous distribution of exponentials like in eq 2, the normalized relaxation spectrum in the frequency domain can be considered to be given through the following expression:[4]

$$\frac{\epsilon''(\omega)}{\epsilon_s - \epsilon_\infty} = \int_{-\infty}^{\infty} \frac{\omega\tau}{1 + \omega^2\tau^2} \varrho(\ln \tau)\, d \ln \tau \quad (3)$$

where $\epsilon''(\omega)$ is the imaginary part of the dielectric constant at frequency ω; ϵ_s and ϵ_∞ are the static dielectric constant and infinite frequency dielectric constant, respectively. The integral in eq 3 is similar to the one in eq 2, although for the former, the kernel in the integral is given in terms of a Lorentzian-like frequency-dependent function instead of an exponential function for the latter. This method of data treatment is advantageous because not only does it give a consistency in analyzing both types of spectroscopic data but also it avoids a parametric model function in curve fitting, which would require an excessively large number of adjustable parameters, and might consequently introduce unwanted errors.

The application of the modified CONTIN program to obtain the distribution function of relaxation times has been previously reported in the literature;[4,14] it has been extensively discussed together with its generalization elsewhere.[15] Nevertheless, some of its applications and generalizations have already been introduced.[5,16,17]

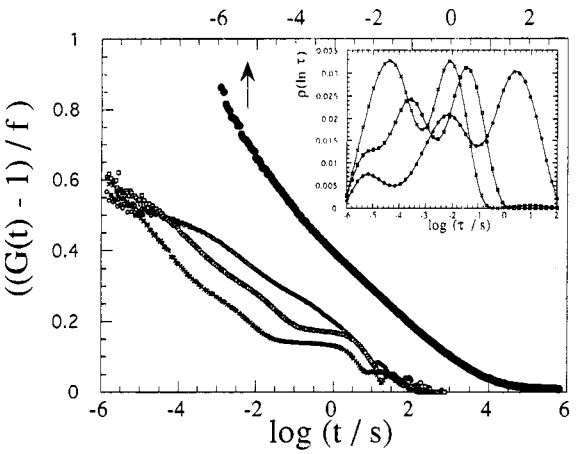

Figure 1. Intensity autocorrelation functions of PIMA homopolymer at 418 (○), 428 (□), and 438 K (×). The autocorrelation function of PMMA homopolymer at 388 K is also included for comparison. In the inset time relaxation distribution functions obtained from the autocorrelation functions of the PIMA homopolymer are shown.

4. Results

4.1. PIMA Homopolymer. Intensity autocorrelation functions measured for the PIMA homopolymer were recorded every 5 K between 418 and 438 K. In Figure 1 we plot the intensity autocorrelation function versus the logarithm of time for the temperatures 418, 428, and 438 K. The experimental measurements clearly show structures indicating that more than one single process is active at these temperatures within the time window of the PCS. These structures are better represented by $\varrho(\ln \tau)$ as calculated by the CONTIN algorithm. The results are plotted in the inset of Figure 1, where one can clearly distinguish at least two main

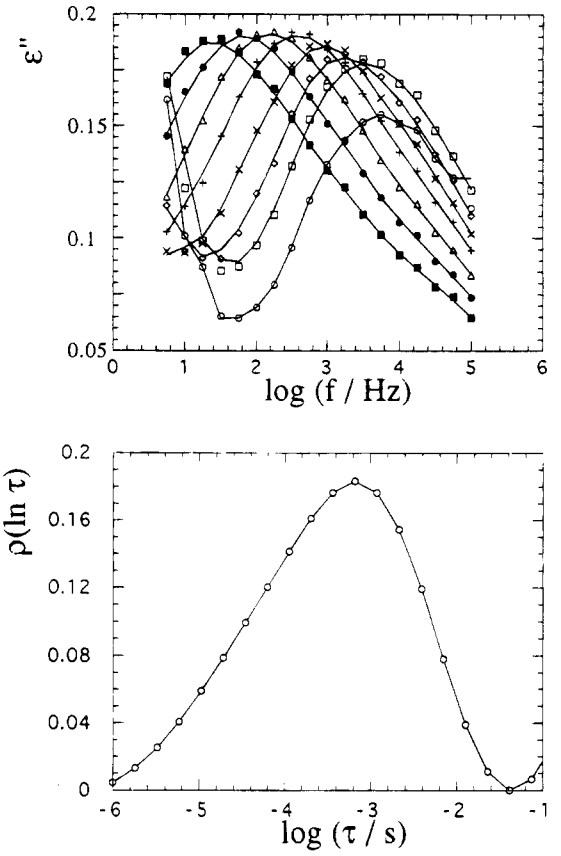

Figure 2. (a) Isothermal dielectric loss peaks for the PIMA homopolymer measured at 465 (○), 460 (□), 455 (◇), 450 (×), 445 (+), 440 (△), 435 (●), and 430 K (■). The lines are drawn to guide the eyes. (b) Relaxation time distribution obtained with the modified CONTIN at 455 K.

processes. Additional structures appear in the short-time region for temperatures at 418 and 428 K. However, due to cut-off effects, it is not clear that the short-time peak for the data at 418 K, which appears as a shoulder in the 428 K case, can be assigned to a true relaxation process. A peak at long times that exhibits the characteristics of long-range fluctuations (cluster)[18] is also present but excluded in the inset of Figure 1. With the availability of $\varrho(\ln \tau)$, one can, in principle, proceed to calculate moments. However, due to overlapping dynamic processes, we believe it to be more reliable to obtain the relaxation time directly from the position of the peak rather than from the calculated moment. Relaxation times thus obtained for the PIMA homopolymer are plotted in Figure 3 together with the dielectric relaxation results presented in the next section. To complement these results, PCS measurements were also carried out on bulk PMMA homopolymer. The dynamics associated with the data in amorphous PMMA is discussed in the literature;[11] here the intensity autocorrelation function of the PMMA homopolymer at 388 K is displayed in Figure 1 for comparison.

The imaginary parts of the isothermal dielectric susceptibilities, ϵ'', measured in the temperature range of 430−465 K with an increment step of 5 K are plotted in Figure 2a. Apart from the conductivity contribution, only one process is observed in the dielectric permittivity in the entire frequency range covered. From the loss peaks and through the modified CONTIN program described above, we have obtained the corresponding distribution functions of relaxation times. A representative distribution function corresponding to that at 455 K omitting the contribution at long times due to

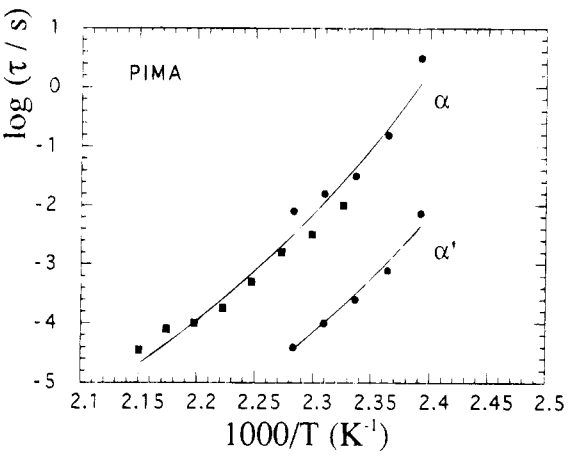

Figure 3. Logarithmic plot of the characteristic relaxation times of the PCS (●) and dielectric (■) data for the PIMA homopolymer. Solid lines are VFHT (eq 4) fits (see the text).

conductivity is shown in Figure 2b. As can clearly be seen and according to the $\epsilon''(\omega)$, only a single peak is involved in $\varrho(\ln \tau)$ obtained from DS. We have extracted the relaxation times from the peak positions of the distribution functions. These times are plotted in Figure 3 along with the values obtained by PCS in this section. The single DS process compares well with the slow relaxation mode of the PCS experiment on bulk PIMA, both exhibiting a strong non-Arrhenius temperature dependence (Figure 3), characteristic of the primary (α) relaxation near T_g. The non-Arrhenius behavior has a fit to a Vogel−Fulcher−Tamman−Hesse (VFTH) equation.

$$\tau = \tau_0 \exp\left(\frac{B}{T - T_0}\right) \tag{4}$$

where, due to the limited temperature range, a fixed τ_0 ($=10^{-13}$ s) value has been assumed. The representation of the α-relaxation times by eq 4 leads to the activation parameters $B = 2481 \pm 143$ K and the ideal glass transition temperature $T_0 = 335 \pm 6$ K. For the fast (α′) relaxation times of the PCS experiment, we have assumed the same τ_0 and T_0 to reduce the number of free parameters. In this case, the fit of eq 4 to the α′-times yields expectedly a low value of the activation parameter ($B = 2023 \pm 13$ K). The probable origin of the fast relaxation process observed only in PCS will be discussed in a later section.

4.2. Random 50% PIMA-PMMA Copolymer. In Figure 4, we show the intensity autocorrelation function measured for the copolymer with composition 50% at 413, 423, and 433 K. To represent the data clearly, we have subtracted a contribution at the long times, which, as mentioned before, is probably due to long-range density fluctuations (cluster scattering) of the material. In the inset of Figure 4, we have plotted the respective relaxation time distribution functions $\varrho(\ln \tau)$ extracted from the intensity correlation functions using the modified CONTIN program (eq 2). Like PIMA homopolymer, more than one single process is present in the dynamical window of the PCS as anticipated from the shape of the experimental $G(t)$. The relaxation times obtained from the peak positions of these distribution relaxation functions are plotted in Figure 6 along with those obtained from the dielectric relaxation technique.

In Figure 5a, we plot the isothermal loss peaks of the dielectric susceptibility in the temperature interval from 300 K up to 426 K with an approximate step of 16 K. A

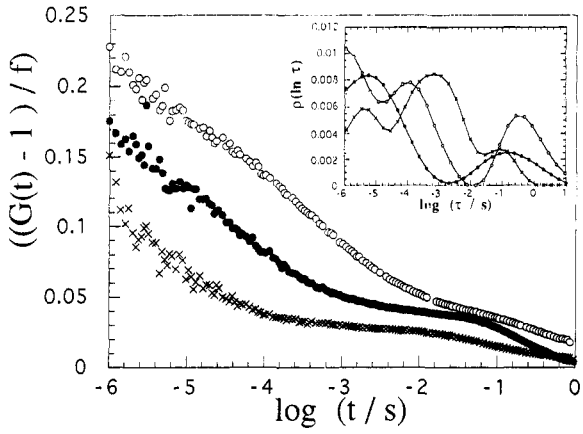

Figure 4. Intensity autocorrelation functions for the 50% PIMA–PMMA copolymer at 413 (○), 423 (●), and 433 K (×). In the inset the corresponding time relaxation distributions are shown.

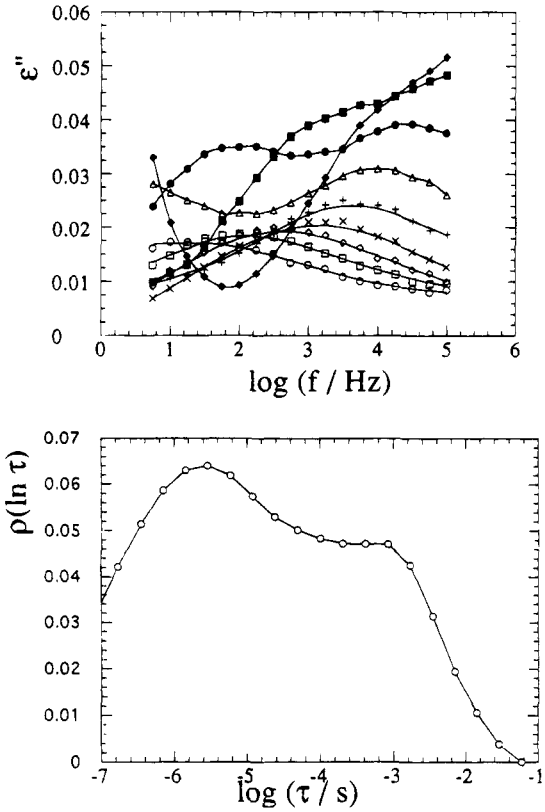

Figure 5. (a) Isothermal loss peaks for the copolymer measured at temperatures 300 (○), 316 (□), 331 (◇), 347 (×), 363 (+), 379 (△), 395 (●), 410 (■), and 426 K (▲). (b) Distribution of relaxation times obtained with the modified CONTIN at 414 K.

representative relaxation time distribution function for the sample at 414 K is shown in Figure 5b. In contrast to PIMA homopolymer, an additional peak is present in Figure 5b (the peak at long times due to conductivity of the material is not included in this plot). At temperatures lower than 414 K, these two peaks are further apart and, hence, can be readily resolved. However, at the lowest temperature studied, one of the relaxation peaks moves outside of the dynamical range of the apparatus. Despite some overlap of the relaxation processes at high temperatures, the characteristic times can be obtained from the maxima of the peaks of $\varrho(\ln \tau)$.

Figure 6 shows the relaxation times of the different processes in the IMA–MMA probed by the PCS and DS

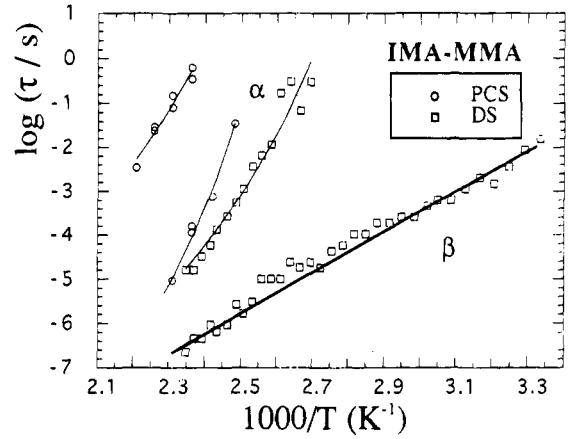

Figure 6. Logarithmic plot of the characteristic relaxation times of the PCS (○) and dielectric (□) data for the copolymer. The thick line stands for the β process of the homopolymer PMMA as taken from ref 22. The other lines are VFHT (eq 4) fits (see the text).

techniques. All processes but the fastest one display strong temperature dependences characteristic for non-Arrhenius behavior. The VFTH equation was therefore used to describe this temperature variation using again a fixed τ_0 (=10^{-13} s). The fitting parameters B and T_0 assume the values $B = 4680 \pm 372$ K and $T_0 = 264 \pm 13$ K for the slow PCS process; $B = 1814 \pm 102$ K and $T_0 = 335 \pm 5$ K for the α-relaxation process as probed by PCS, whereas $B = 2856 \pm 180$ K and $T_0 = 275 \pm 7$ K for the α-dielectric (slow) mode. Unlike the situation in homopolymers[5–7] (see also Figure 3), the α-relaxation times in the IMA–MMA copolymer probed by PCS and DS do not coincide even though the underlying molecular mechanism is expected to be common for the dynamics of both density and orientation fluctuations. Either this is a hint of translation–rotation decoupling at low temperatures[19–21] or an additional process in the DS experiment is unclear. Phenomenologically, the α-relaxation time of the density correlation function (PCS experiment) conforms to the average local mobility of the mixed system since it falls between the values of the α-relaxation time in the bulk homopolymers (see Figure 8a).

Alternatively, the relaxation times of the fast DS process compare well with the secondary β-relaxation in bulk PMMA,[11,22] whereas this process is absent in the PIMA homopolymer. This fact becomes apparent in Figure 7 which displays normalized dielectric losses in the IMA–MMA copolymer and PIMA homopolymer at constant frequency and different temperatures. The absence of a dielectric secondary process in the PIMA homopolymer seems to be reminiscent of the separation between the α- and β-relaxations in poly(alkyl methacrylate)s where, for the high members of the series, only a single merged $\alpha\beta$ process, bearing similarities to the α-process, is observed.[22–24] Similarly, the β-relaxation is considerably suppressed by introducing a bulkier side group.[25]

Summing up, the random PIMA–PMMA copolymer reveals rich dynamic behavior. As seen in Figure 6, besides the secondary relaxation peak associated with PMMA segments which is active in both PCS and DS, the intermediate process in PCS and the slow mode in DS reflect the primary (α) relaxation in the mixed glass.

5. Discussion

The dynamic complexity of the random copolymer and the constituent homopolymers is clearly seen from the

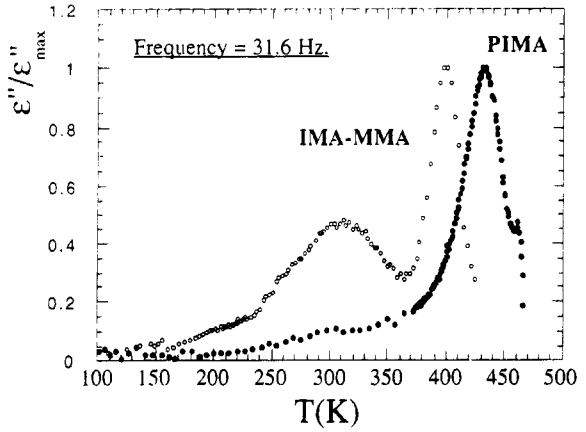

Figure 7. Plot of the normalized loss peaks versus temperature measured at a fixed frequency of 31.6 Hz. Open circles stand for the copolymer and solid ones for the homopolymer.

mere inspection of the multiplicity of peaks as resolved by DS and PCS (Figures 3 and 6). Forced miscibility at local (0 nm) scale via copolymerization should be reflected in a single α-relaxation process intermediate between the two homopolymers,[26-28] the presence of a single T_g in the copolymer indicates that the range of homogeneity is greater than about 10 nm. To compare the relaxation processes between copolymer and homopolymers, we plot in Figure 8a the relaxation times versus temperature for the homopolymers and copolymer. In Figure 8a, one notes the closeness of the fast β-relaxation in PMMA and IMA–MMA copolymer observed by DS[22] and PCS.[11] This peak is insensitive to the variation of the local structure, which is anticipated from the independence of the β-relaxation on free volume.[29,30] Thus, we can identify the fast relaxation process in the copolymer to be associated with the β-relaxation of PMMA glass. The ratio $\epsilon_\beta''/\epsilon_\alpha''$ of the maximum losses for β- and α-processes is about 0.7 for PMMA and 0.5 for the copolymer (Figure 7). Provided that the ϵ_α'' values for the bulk homopolymers are similar, the β-relaxation appears to be enhanced in the copolymer, probably due to some plasticization effect.[29] While the volume fluctuations are not sufficiently large to allow for secondary β-relaxation in bulk PIMA, mixing with PMMA appears to promote these fluctuations. It seems reasonable that the fast relaxation in PMMA and the copolymer melt (measured by both PCS and DS) can be assigned to the same phenomenon.

The assignment of the other processes is less straightforward. For PIMA homopolymer, density fluctuations relax with two mechanisms, whereas segmental orientation fluctuations probed by DS exhibit a single relaxation process (solid circles in Figure 8a). The peak obtained in DS is similar to the slow relaxation mode of the density fluctuations detected by the PCS experiment (solid squares in Figure 8a). Based on its strong temperature dependence, this mode can be assigned to the primary α-relaxation. Hence, both experimental techniques appear to probe the same glass transition process.[6,7] Unlike the β-relaxation, the α-relaxation time depends strongly on the available free volume (or $T - T_g$) and should therefore become faster in the copolymer which has a lower T_g. In fact, as shown in Figure 8a for the copolymer, both dielectric and light scattering α-processes are faster than the corresponding single α-process in the PIMA homopolymer. There is, however, some uncertainty between the α-relaxation times as measured by PCS and DS in copolymer. This disparity could be due to the errors introduced in the

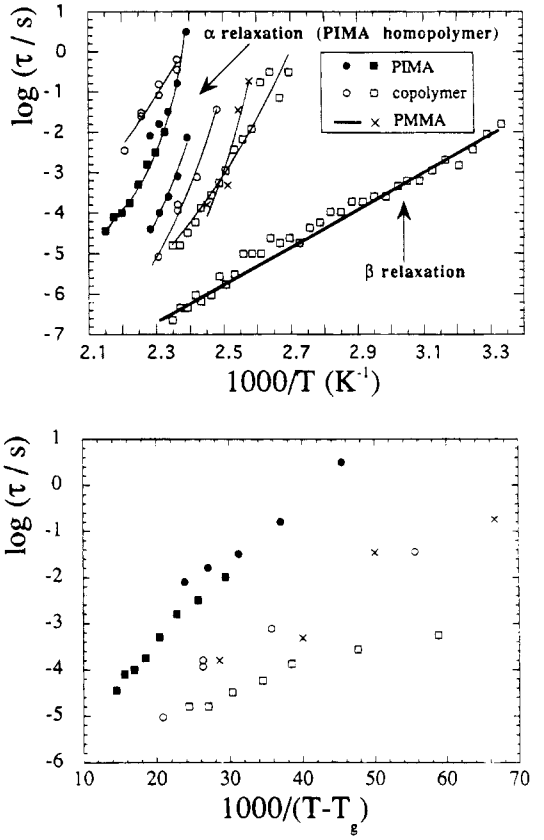

Figure 8. (a) Plot of all relaxation times versus inverse temperature. Solid points correspond to PIMA homopolymer and the open ones to the copolymer. Circles are from PCS measurements, and squares are from dielectric relaxation. Crosses are α-relaxation times from PCS measurements on PMMA. The thick line stands for the β-dielectric process of PMMA. The other lines are VFHT fits (eq 4). (b) Plot of the relaxation times of part a, with the temperature shifted by the respective T_g values of each sample. Points corresponding to the β-dielectric process of PMMA have been omitted. The identification of the symbols are the same as those used in part a.

extraction of the relaxation times from overlapping peaks. However, it is also possible that dynamic heterogeneities in the mixed poly(IMA–MMA) glass might be emphasized differently by the two techniques. A double α-relaxation in a calorimetrically and rheologically compatible mixture, i.e., a single T_g and a single mechanical peak, is not infeasible due to the short length scale (0 nm) of the primary α-relaxation provided that the difference in the individual mobilities is sufficiently large.[26,27] The disparity in the mobilities is mainly determined by the difference in the T_g of the two components which, in the present case, is rather small.

It is useful to compare the α-relaxation times in the copolymer and constituent homopolymers at temperatures equidistant to T_g. Figure 8b was constructed by using T_g = 373 K for PMMA, T_g = 396 K for PIMA, and T_g = 380 K for the copolymer. It is apparent from Figure 8b that α-relaxation in bulk PIMA probed by both PCS and DS (solid circles and squares) is slower than that in the copolymer; this is probably due to the greater stiffness of the PIMA chain.[2] In the copolymer the α-relaxation is rather similar to the PMMA component that possesses higher mobility than PIMA at temperatures equidistant to T_g. Disparity in the components mobilities along with thermodynamic interactions might lead to nanoheterogeneities and, hence, two distinct α-processes in macroscopically homogeneous systems.[31]

In addition to the α- and β-relaxation peaks that are clearly assigned in the present systems, PCS provides a strong evidence of two extra modes; a fast relaxation (α′) mode in PIMA (Figures 3 and 8a) and a slow one in copolymer (Figures 6 and 8a); these modes appear to be dielectrically inactive. For bulk PIMA, the new α′-relaxation shows a strong T-dependence, reminiscent of the glass transition process. This mode is, however, absent in bulk PMMA and can hardly be seen in the copolymer. Based on these findings, this fast mode observed in PIMA homopolymer is possibly related to rotational motion of the rigid isobornyl group around the C–O bond that could also affect local density fluctuations. In amorphous side-chain polymers, e.g., poly(n-hexyl methacrylate)[32] and poly(lauryl methacrylate),[24] the dynamics of long side chains are found to decouple from the α-relaxation peak associated with the cooperative motion of the main-chain backbone.

For IMA–MMA copolymer, the slow relaxation of the PCS experiment has a rather narrow distribution of relaxation times (Figure 4) and is also the slowest process in the system (Figure 8a). Concentration fluctuations are possible for the present copolymer system. As recently reported,[33,34] a diblock copolymer melt can display a slow diffusive relaxation arising from intrinsic composition fluctuations. It might be possible to ascribe the slow extra mode in IMA–MMA random copolymer to concentration fluctuations. In fact, the extremely large value of the activation parameter B (=4680 K) (eq 4) is due to the fixed small intercept τ_0 ($=10^{-13}$ s) appropriate for local segmental times but not for diffusive times over a large distance.

6. Concluding Remarks

In systems more complex than simple amorphous homopolymers, the description of the characteristic features of the glass transition is a pertinent issue and additional questions derived from the complexity of the problem arise. In such multicomponent systems like copolymers or blends, the main difficulty relates to the dynamic inhomogeneity, i.e., to what extent a single mixed behavior occurs or whether the components preserve dynamic individualities.

The method of analysis as presented is proven to be adequate in treating these kinds of data, for which traditional analysis based in parametric fitting functions is ambiguous. We have modified the CONTIN program to obtain distributions of relaxation times directly from the experimental data without using any additional hypothesis. These distributions can be obtained not only from the PCS data but also from the dielectric relaxation data, even for such a complex system as the 50% PIMA–PMMA which, as shown, presents a fairly rich dynamical behavior. In this way, our method treats the time dependence and frequency dependence data consistently and obtains useful physical information from the experimental data. Thus, we have been able to discuss possible molecular origins of a multiplicity of relaxation processes appearing in the present system and show that unique results of interest can be derived from the study of segmental dynamics in copolymers.

Acknowledgment. The authors acknowledge financial support from EC, HCM-Network project Contract ERBCHRXCT920009. J.C. and F.A. also acknowledge partial financial support from Gipuzkoako Foru Aldundia. J.C., F.A., and C.H.W. also acknowledge the NATO project CRG-940012.

References and Notes

(1) Zhang, X. Q.; Wang, C. H., unpublished results.
(2) Hadjichristidis, N.; Mays, J.; Ferry, W.; Fetters, L. J. *J. Polym. Sci., Polym. Phys.* **1984**, *22*, 1745.
(3) Zhang, X. Q.; Wang, C. H. *J. Polym. Sci., Polym. Phys.* **1994**, *31*, 1799.
(4) Alvarez, F.; Colmenero, J.; Fytas, G. *Prog. Colloid Polym. Sci.* **1993**, *91*, 20.
(5) Alvarez, F.; Colmenero, J.; Kanetakis, J.; Fytas, G. *Phys. Rev. B* **1994**, *49*, 21, 14996.
(6) Boese, D.; Meier, G.; Kremer, F.; Hagenah, J.-U.; Momper, B.; Fischer, E. W. *Macromolecules* **1989**, *22*, 4416.
(7) Kanetakis, J.; Fytas, G.; Kremer, F.; Pakula, T. *Macromolecules* **1992**, *25*, 3484.
(8) Alegría, A.; Colmenero, J.; Nagi, K. L.; Roland, C. M. *Macromolecules* **1994**, *27*, 4486.
(9) Chung, G. C.; Kornfield, J. A.; Smith, S. D. *Macromolecules* **1994**, *27*, 964.
(10) Zawada, J. A.; Ylitabo, C. M.; Fuller, G. G.; Colby, R. H.; Long, T. E. *Macromolecules* **1992**, *25*, 8896.
(11) Fytas, G.; Wang, C. H.; Fischer, E. W. *Macromolecules* **1988**, *21*, 2253.
(12) Wang, C. H.; Fytas, G.; Lilge, D.; Dorfmuller, Th. *Macromolecules* **1981**, *14*, 1363.
(13) Provencher, S. W. *Comput. Phys. Commun.* **1982**, *27*, 213.
(14) Karatasos, K.; Anastasiadis, S. H.; Semenov, A. N.; Fytas, G.; Pitsikalis, M.; Hadjichristidis, N. *Macromolecules* **1994**, *27*, 3543.
(15) Alvarez, F.; Alegría, A.; Colmenero, J. *J. Chem. Phys.* **1995**, *103*, 798.
(16) Alvarez, F. Ph.D. Thesis, Universidad del País Vasco (UPV/EHU), San Sebastián, Spain, 1993.
(17) Alvarez, F.; Alegria, A.; Colmenero, J., to be submitted.
(18) Fischer, E. W. *Physica A* **1993**, *201*, 183.
(19) Fujara, F.; Geil, B.; Sillescu, H.; Fleischer, G. Z. *Phys. B* **1992**, *88*, 195.
(20) Rössler, E.; Eierman, P. *J. Chem. Phys.* **1994**, *100*, 5237.
(21) Cicerone, M. T.; Blackburn, F. R.; Ediger, M. D. *J. Chem. Phys.* **1995**, *102* (1), 471.
(22) McCrum, N. G.; Read, B. E.; Williams, G. *Anelastic and Dielectric Effects in Polymeric Solids*; Wiley: London, 1967.
(23) Williams, G.; Watts, D. C. *Trans. Faraday Soc.* **1971**, *67*, 2793.
(24) Floudas, G.; Placka, P.; Stepanek, P.; Brown, W.; Fytas, G.; Ngai, K. L. *Macromolecules*, submitted.
(25) Floudas, G.; Fytas, G.; Fischer, E. W. *Macromolecules* **1991**, *24*, 1955.
(26) Fytas, G.; Anastasiadis, S. H. In *Disorder Effects on Relaxation Processes*; Richert, R., Blumen, A., Eds.; Springer-Verlag: Berlin, 1994.
(27) Zetsche, A.; Fischer, E. W. *Acta Polym.* **1994**, *45*, 168.
(28) Roland, C. M.; Ngai, K. L. *Macromolecules* **1991**, *24*, 5315.
(29) Fischer, E. W.; Hellman, G. P.; Spiess, H. W.; Hörtes, H. W.; Ecarius, U.; Wehle, M. *Makromol. Chem. Suppl.* **1985**, *12*, 189.
(30) Rizos, A. K.; Fytas, G.; Ma, R. J.; Wang, C. H.; Abetz, V.; Meyer, G. C. *Macromolecules* **1993**, *26*, 1869.
(31) Khokhlov, A.; Emkhimovich, I. *Macromolecules* **1993**, *26*, 7195.
(32) Meier, G.; Kremer, F.; Rizos, A.; Fytas, G. *J. Polym. Sci., Polym. Phys.*, in press.
(33) Giebel, L.; Meier, G.; Fytas, G.; Fischer, E. W. *J. Polym. Sci.* **1992**, *30*, 1291.
(34) Anastasiadis, S. H.; Fytas, G.; Vogt, S.; Fischer, E. W. *Phys. Rev. Lett.* **1993**, *70*, 2415; *Macromolecules* **1994**, *27*, 4335.

MA946378X